Fig. 7. Effect of outer dielectric thickness D_o ($\epsilon_d = 5.24$).

TABLE I
SEPARATE COMPUTATIONS TO SHOW THE AGREEMENT OF
 $F_o/B.W.$ AND Q -FACTOR

$N \times 10^{18} \text{ m}^{-3}$	1	2	3	4	5	6
TEM $F_o/B.W.$	17.76	76.60	242.0	635.5	1477	3132
TEM Q	18.86	76.22	245.0	633.9	1476	3140
TE_{10} $F_o/B.W.$	35.12	126.5	370.0	930.7	2106	4383
TE_{10} Q	35.88	125.0	366.2	926.2	2100	4375

Note: Results for both TEM and TE_{10} cases are presented for the filter with $D_d = 1 \text{ cm}$, $D_p = 0.8 \text{ cm}$, and $\epsilon_d = 5.24$

increased. Thus more energy will be stored within the central dielectric slab to enhance the corresponding Q -factor and to reduce the bandwidth as D_p or N is increased.

Illustrated in Fig. 7 are the curves to demonstrate the effect of varying the thickness D_o of the outer dielectric slabs. The center frequency is indeed determined by the thickness of the central dielectric slab by comparing the curve for $D_o = 0$ with those for other D_o 's. As shown, the variation of D_o has little effect on the center frequency. On the contrary, the magnitude of D_o still has considerable influence on the bandwidth, although its effect is not regular.

An actual plasma always exhibits losses whose relative dielectric constant may be expressed as [7]

$$\epsilon_p = \epsilon'_p - j\epsilon''_p \quad (6)$$

where

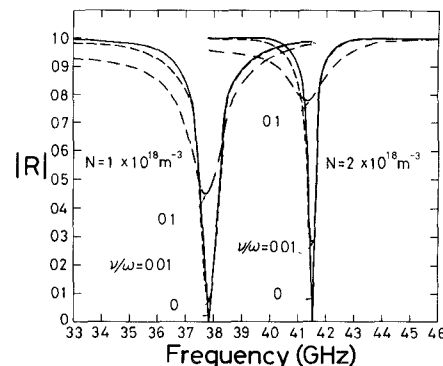
$$\epsilon'_p = 1 - \frac{\omega_p^2 / \omega^2}{1 + (\nu / \omega)^2} \quad (7)$$

$$\epsilon''_p = \frac{(\omega_p / \omega)^2 (\nu / \omega)}{1 + (\nu / \omega)^2} \quad (8)$$

Here, ϵ''_p accounts for losses in plasma and ν is the collisional frequency between electrons and molecules or ions. Fig. 8 presents curves (for the TE_{10} case) to characterize the lossy effect with ν / ω as a parameter. The complete transmission window is found to disappear when a loss is introduced, and the reflection becomes pronounced as ν / ω becomes large.

IV. CONCLUSIONS

A phenomenon of having complete transmission in some frequencies and large reflection in other frequencies has been utilized

Fig. 8. Illustration of lossy effect for $D_d = 1.0 \text{ cm}$, $D_p = 0.8 \text{ cm}$, and $\epsilon_d = 5.24$ (TE_{10} case).

to implement a new tunable bandpass filter in a microwave regime. Many useful results for specifying the filter performance have been presented and investigated in detail.

The new filter is analyzed based on a simple model of cold plasma. Hence, an experimental work is definitely needed as a future study in complementing the simplified theory developed in this study.

The leaky resonance phenomenon may be useful in constructing other new devices for special purposes, e.g., as an on-off switch or a modulating device. The characteristics of the plasma-dielectric structure may also be tuned externally by applying a steady magnetic field across the plasma.

ACKNOWLEDGMENT

Discussions with Prof. H. J. Li and S. K. Jeng were helpful and much appreciated.

REFERENCES

- [1] G. C. Tai, Y. W. Kiang, and C. H. Chen, "Plasma-dielectric sandwich structure used as a tunable microwave filter," in *Proc. 1982 Int. IEEE/APS Symp. Nat. Radio Sci. Meet. Nucl. Electromagn. Pulse Meet.* (University of New Mexico, Albuquerque), May 1982, pp. 103-106.
- [2] C. H. Chen and Y. W. Kiang, "A variational theory for wave propagation in a one-dimensional inhomogeneous medium," *IEEE Trans. Antennas Propagat.*, vol. AP-28, pp. 762-769, Nov. 1980.
- [3] E. Bahar and B. S. Agrawal, "Transmission of horizontally polarized waves and trapped waveguide modes in inhomogeneous media," *IEEE Trans. Antennas Propagat.*, vol. AP-25, pp. 807-813, Nov. 1977.
- [4] N. A. Krall and A. W. Trivelpiece, *Principle of Plasma Physics*. New York: McGraw-Hill, 1973.
- [5] J. A. Kong, *Theory of Electromagnetic Waves*. New York: Wiley, 1975.
- [6] R. W. Daniels, *An Introduction to Numerical Method and Optimization Technique*. New York: Elsevier North-Holland, 1978.
- [7] K. C. Yeh and C. H. Liu, *Theory of Ionospheric Waves*. New York: Academic Press, 1972.

Dielectric Waveguide Corner and Power Divider with a Metallic Reflector

KAZUHIKO OGUSU, MEMBER, IEEE

Abstract—The right-angle corner and T- and Y-junction-type power dividers with the metallic reflector are experimentally investigated which are useful for dielectric waveguide millimeter-wave integrated circuits.

Manuscript received December 29, 1982; revised August 10, 1983.

The author is with the Faculty of Engineering, Shizuoka University, Hamamatsu, 432 Japan.

These devices have been fabricated from the rectangular dielectric image line and have been tested in the 20–26-GHz range. The tested corner exhibits the bending losses 1.0–1.75 dB for single-mode operation and 0.23–0.7 dB for multimode operation. The tested Y-junction-type power divider exhibits the power division of about 4.4 dB and the isolation is above 20 dB. The metallic reflector can be applied to other passive components.

I. INTRODUCTION

Millimeter-wave integrated circuits using dielectric waveguides [1], [2] have been extensively investigated under the stimulus of the rapid development of integrated optics [3]. Millimeter-wave dielectric waveguides are usually made of plastic, high-purity alumina, high-resistivity semiconductors such as Si, GaAs, and ferrite. In the future, semiconductors and ferrite will be more widely used for realizing the active and nonreciprocal devices. A bending structure is an essential component in integrated circuits. However, it is difficult to form the curved structure made of semiconductors, ferrite, etc. by machining, which is commonly used. In addition, a radiation loss is always present at the curved section, since the dielectric waveguide is an open structure. In order to decrease the bending loss, one must make the bending radius large. This often comes into question in practical applications.

One way to overcome these problems is to use a reflector instead of the curved section. The basic idea of the corner with the reflector has already been proposed by King [4]. Although its principle is very simple, the properties have not been sufficiently investigated.

This short paper discusses the right-angle corner with the reflector and proposes the T- and Y-junction-type power dividers as a variation of the corner with the reflector. The experiments are conducted in the *K*-band. The corner and power divider with the reflector seem to be practical in millimeter-wave integrated circuit applications from the standpoint of low loss, size, and ease of fabrication.

II. PRINCIPLES OF OPERATION AND EXPERIMENTAL METHODS

In this section, we describe the principles of operation of the corner and power divider with the metallic reflector and a method for measuring their losses. Fig. 1 shows the geometries of the right-angle corner and T-junction-type power divider, and the experimental setup. The waveguide used in this short paper is a rectangular dielectric image line made of polypropylene ($\epsilon_r = 2.25$).

The corner with the reflector is based on the principle similar to an optical mirror. The reflector is placed at 45° with each waveguide axis. The fundamental E_{11}^y mode is excited through a metal waveguide system and the insertion loss is measured. The bending loss of the corner can be obtained by comparison of the insertion loss of the bent waveguide shown in Fig. 1 (c) with that of a straight waveguide of identical length (40 cm). The bending loss includes the radiation loss, mode conversion loss, and the return loss toward the input port. Strictly speaking, the dielectric loss and conductor loss cannot be perfectly isolated from the measured loss since the field distribution of the bent waveguide is not identical with that of the straight waveguide in the neighborhood of the corner. Therefore, the bending loss contains these discrepancies too. In our experiments, to increase the accuracy of measurements, two straight sections and a corner section were separately formed and were fixed on a ground plane with adhesive tape. When the location of the reflector is changed, only the corner section is exchanged. The loss at the junction between the

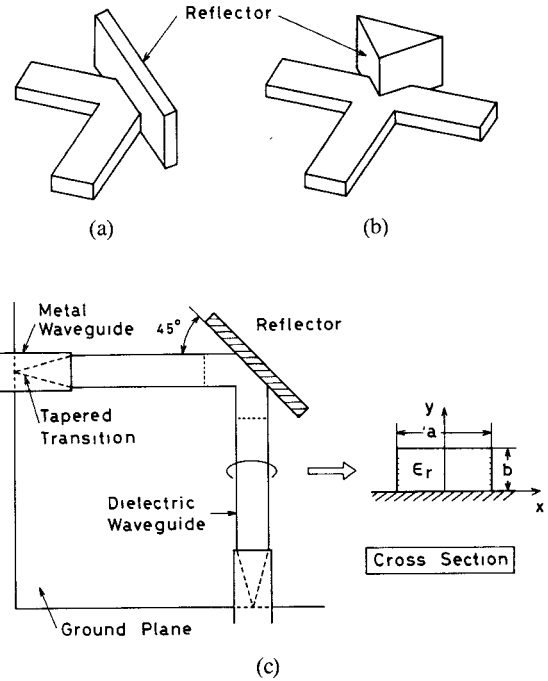


Fig. 1. (a) Corner with the reflector. (b) T-junction-type power divider with the reflector. (c) Measurement setup for determining the bending loss of the corner.

straight and corner sections has been measured to be negligibly small. The additional loss caused by the adhesive tape is about 0.7 dB/m. This value was determined from the difference between insertion losses with and without the tape.

The principle of operation of the power divider with the reflector is as follows. The millimeter-wave power incident at the input port is equally reflected into two output ports by the metallic wedge with a 90° angle. The ratio of the output power to the input power depends on the insertion depth of the wedge. The millimeter-wave incident at one output port is effectively reflected into the input port and the remaining power is transmitted to the other output port. In addition, the radiation, mode conversion, and the reflection toward the millimeter-wave source take place. The isolation between output ports increases as the insertion depth of the wedge becomes large. For operation of this type of power divider, all of the ports must be terminated appropriately.

The attenuation of the power divider is measured in a similar way. However, the absorber (tapered polystyrene foam containing carbon) is attached to the image line of the untested port to achieve the reflection-free termination. Little influence of the reflection on measurements was confirmed by changing the location of the absorber.

III. RESULTS AND DISCUSSION

The corners and power dividers were fabricated from image lines with different cross sections and tested in the 20–26-GHz range using a mechanically tuned Gunn oscillator. The thicknesses b of the waveguide used in the experiments are 3 and 5 mm, and the aspect ratio $a/2b$ is 1.2. The waveguide with $b = 3$ mm (case *A*) supports only the fundamental E_{11}^y mode, whereas the waveguide with $b = 5$ mm (case *B*) supports the E_{11}^y , E_{21}^y , E_{12}^y , and E_{12}^x modes.

Fig. 2 shows the bending loss of the right-angle corner as a function of the location of the reflector. Although King [4] has pointed out that the optimum location of the reflector is at the

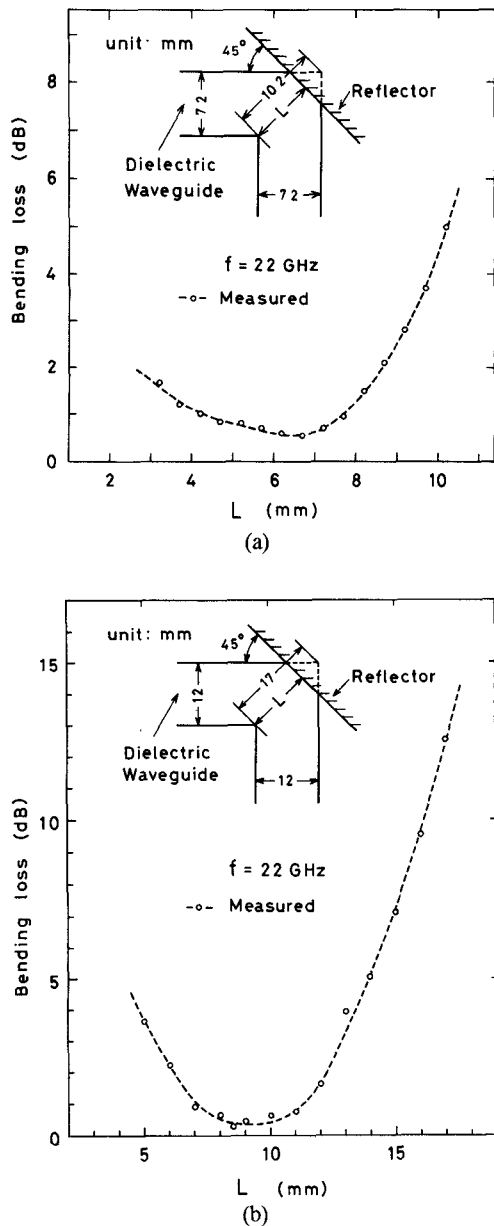


Fig. 2. Bending loss of the corner with the reflector as a function of the location of the reflector. (a) Single-mode operation. (b) Multimode operation.

intersection of the two waveguide axes, strictly speaking, this is not correct. The optimum location is about 1.5 mm away from the intersection for the single-mode corner, and about 1 mm away for the multimode corner. Fig. 2 shows also that the location is not too critical when attempting to achieve minimum loss.

Fig. 3 shows the measured performance of the right-angle corner with the reflector. The reflector is placed at the intersection of the two waveguide axes. The insertion losses of the straight waveguide, including the loss at the transition between the metal waveguide and image line, were 2.22–3.22 dB for case A, and 2.43–2.92 dB for case B. The bending loss of the corner operated in the single-mode region is greater than that of the corner operated in the multimode region.

We compare the bending loss of the corner with that of the curved waveguide measured by Solbach [5]. Although the operating frequency and waveguide parameters in our experiments are different from those in his experiment, the aspect ratios and

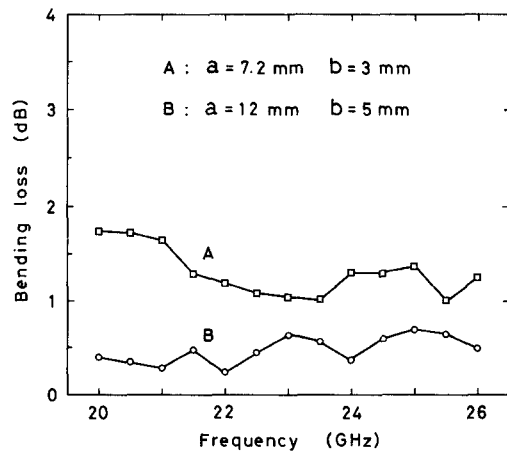


Fig. 3. Measured performance of the right-angle corner with the reflector.

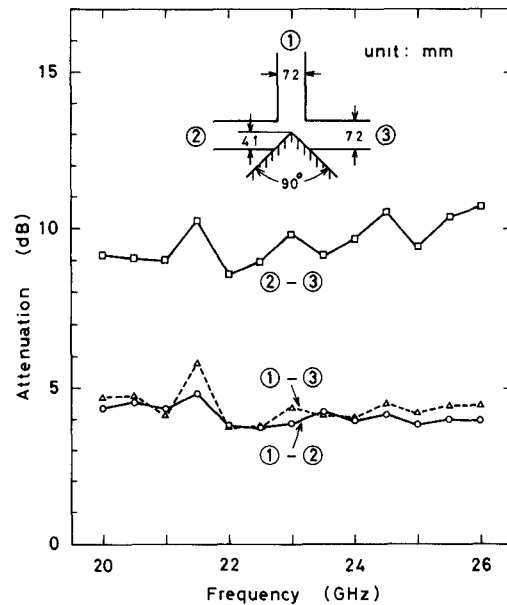


Fig. 4. Measured performance of the T-junction-type power divider with the reflector.

dielectric constants of both waveguides resemble each other. In this case, the waveguide is characterized by the normalized frequency $4\sqrt{ab}/2\sqrt{\epsilon_r-1}/\lambda$. Although this normalization in terms of the equal cross section [6] is not in agreement with the commonly used one ($4b\sqrt{\epsilon_r-1}/\lambda$), it is appropriate for a small aspect ratio ($a/2b \approx 1$). If the waveguide of case A is transformed to the waveguide ($a/2 = b = 2.4$ mm, $\epsilon_r = 2.22$) shown in Fig. 2 of Solbach's paper, the corresponding frequency range becomes 27.7–36.0 GHz. It is found that the bending loss of the corner with the reflector is comparable to that of the curved waveguide of large bending radius R ($R/(a/2) > 10$).

Fig. 4 shows the measured performance of the T-junction-type power divider with the reflector. The top view of the structure is shown in the inset in Fig. 4. The vertex of the wedge is located 0.5 mm inside from the intersection of the three waveguide axes to increase the isolation. The average attenuation between the input and output ports ($(1) - (2)$ and $(1) - (3)$) is 4.26 dB, and the isolation between the output ports ($(2) - (3)$) is greater than 8.5 dB. The perfect power division is equal to 3 dB. Although the isolation of this type of power divider is not very high, we expect that the Y-junction geometry increases the isolation.

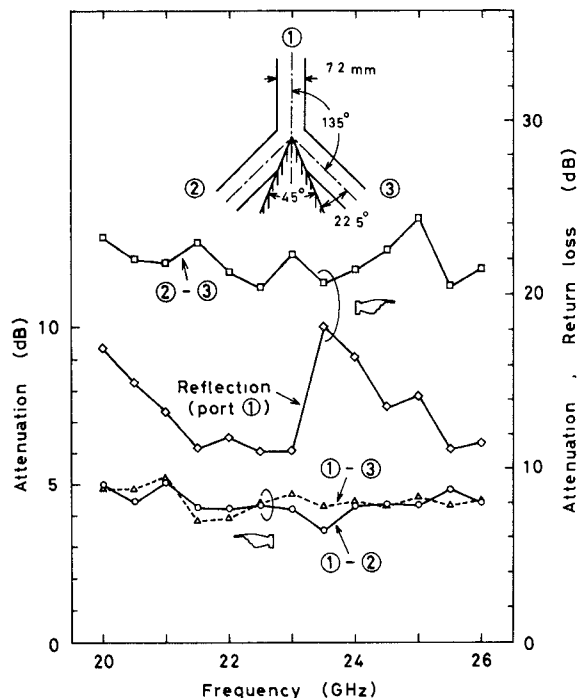


Fig. 5. Measured performance of the Y-junction-type power divider with the reflector.

Fig. 5 shows the measured performance of the Y-junction-type power divider with the reflector. The top view of the structure is shown in the inset in Fig. 5. In this example, the waveguide axes of output ports are inclined at 45° to that of the input port. The vertex of the wedge is located at the intersection of the three waveguide axes, and each face of the wedge is placed at 22.5° with the output waveguide. The average power division is 4.42 dB, and the isolation is greater than 20 dB. Although the isolation is improved, the power division is not improved unexpectedly. The performance of this type of power divider depends on the angle between output waveguides. It seems that the power divider with small output angle exhibits good performance. The reason why the power division was not improved has not been made clear at the present stage. The reflection characteristics at the input port are also shown in Fig. 5. The cause of the difference between experimental and ideal power divisions is considered to be due to the radiation, since the reflection is small (return loss > 10 dB).

IV. CONCLUSION

The corners and power dividers with the metallic reflector have been fabricated from the rectangular dielectric image line and have been tested in the 20–26-GHz range. It is found that the bending loss of the corner with the reflector is comparable to that of the curved waveguide of large bending radius. The proposed Y-function-type power divider exhibits good performance. The metallic reflector can be applied to other passive components for dielectric waveguide millimeter-wave integrated circuits.

REFERENCES

- [1] T. Itoh, "Dielectric waveguide-type millimeter-wave integrated circuits," *Infrared and Millimeter Waves*, vol. 4, K. J. Button and J. C. Wiltse, Ed. New York: Academic Press, 1981, ch. 5.
- [2] R. M. Knox, "Dielectric waveguide microwave integrated circuits—An overview," *IEEE Trans. Microwave Theory Tech.*, vol. MTT-24, pp. 806–814, Nov 1976
- [3] T. Tamir, *Integrated Optics*. Berlin: Springer-Verlag, 1975
- [4] D. D. King, "Properties of dielectric image lines," *IRE Trans. Microwave Theory Tech.*, vol. MTT-3, pp. 75–81, Mar. 1955.
- [5] K. Solbach, "The measurement of the radiation losses in dielectric image line bends and the calculation of a minimum acceptable curvature radius," *IEEE Trans. Microwave Theory Tech.*, vol. MTT-27, pp. 51–53, Jan. 1979.
- [6] W. Schlosser and H. G. Unger, "Partially filled waveguides and surface waveguides of rectangular cross section," *Advances in Microwaves*, vol. 1, L. Young, Ed. New York: Academic Press, 1966, pp. 319–387.

Broadside-Coupled Slot-Line Field Components

RAINEE NAVIN SIMONS, MEMBER, IEEE

Abstract—This paper presents expressions for the odd- and even-mode electric field components and also the magnetic field components in the air, overlay, and dielectric regions of the broadside-coupled slot-line structure. These expressions are numerically computed, and the fields in the cross section and the longitudinal section are illustrated. The surface current distribution on the metal surfaces are also illustrated.

I. INTRODUCTION

The slot-line on a dielectric substrate [1] is a very useful transmission line for realizing nonreciprocal MIC components [2]–[5]. Recently, Cohn [6] has presented the electric and magnetic field components in the dielectric and air regions of a single slot-line. Besides, Simons and Arora [7] have presented expressions for the odd- and even-mode electric field components and the magnetic field components in the air and dielectric regions of an edge-coupled slot-line.

In this paper, expressions for the odd- and even-mode electric field components, and also the magnetic field components in the dielectric and air regions of a suspended broadside-coupled slot-line with an overlay [8], are presented. The dielectric substrate and the overlays are assumed to be isotropic and homogeneous and are of arbitrary thickness and relative permittivity. The conducting cover and the zero-thickness metallization on the substrate are assumed to have infinite conductivity. These expressions are numerically computed at various points in the dielectric region and the air regions of the structure. The odd- and even-mode electric field, the magnetic field in the cross section, and the odd- and even-mode magnetic field in the longitudinal section through the slot are illustrated. Besides, the current distribution on the metal surfaces and the magnetic field tangential to the metal surfaces are illustrated. Finally, a slot-line with a lower ground plane is considered. The current paths on the lower ground plane and the magnetic field tangential to the lower ground plane are illustrated.

II. DERIVATION OF THE FIELD COMPONENTS

The suspended broadside-coupled slot-line with an overlay is illustrated in Fig. 1(a). For the case of even excitation, a magnetic wall is placed along the plane of symmetry. It then suffices to restrict the analysis to the upper half of the structure (Fig. 1(b)). A similar simplification is possible for the case of odd excitation, except that the magnetic wall at the plane of symmetry is replaced by an electric wall (Fig. 1(b)). As in the earlier analysis

Manuscript received March 23, 1983; revised August 3, 1983.

R. N. Simons is with the Centre for Applied Research in Electronics (CARE), Indian Institute of Technology Delhi, Hauz Khas, New Delhi-110016, India.